BRNO UNIVERSITY OF TECHNOLOGY

Faculty of Electrical Engineering
and Communication

BACHELOR'S THESIS

Brno, 2019 Rastislav Čermák

BRNO UNIVERSITY OF TECHNOLOGY

VYSOKÉ UČENÍ TECHNICKÉ V BRNĚ

FACULTY OF ELECTRICAL ENGINEERING AND COMMUNICATION

FAKULTA ELEKTROTECHNIKY
A KOMUNIKAČNÍCH TECHNOLOGIÍ

DEPARTMENT OF MICROELECTRONICS

ÚSTAV MIKROELEKTRONIKY

INVESTIGATION OF PROPERTIES OF CDTE SINGLE-CRYSTALS SURFACES WITH SUB-NANOMETER DEPTH RESOLUTION

STUDIUM VLASTNOSTÍ POVRCHU MONOKRYSTALŮ CDTE SE SUB-NANOMETROVÝM HLOUBKOVÝM ROZLIŠENÍM

BACHELOR'S THESIS
BAKALÁŘSKÁ PRÁCE

AUTHOR
AUTOR PRÁCE

Rastislav Čermák

SUPERVISOR
VEDOUCÍ PRÁCE

Ing. Ondřej Šik, Ph.D.

BRNO 2019

BRNO UNIVERSITY OF TECHNOLOGY
FACULTY OF ELECTRICAL ENGINEERING AND COMMUNICATION

Bachelor's Thesis

Bachelor's study field **Microelectronics and Technology**
Department of Microelectronics

Student: Rastislav Čermák ***ID:*** 198143

Year of study: 3 ***Academic year:*** 2018/19

TITLE OF THESIS:

Investigation of properties of CdTe single-crystals surfaces with sub-nanometer depth resolution

INSTRUCTION:

The aim of the thesis is investigation of the uppermost atomic layers of CdTe single crystals by the Low Energy Ion Scattering technique after various methods of the surface processing. This work is focused on comparison of etching effects on polar, Te-terminated 111(B) and Cd-terminated 111(A) crystallographic orientations of the crystal. Another goal of the work is in situ analysis of the effect of exposure of the crystal to atomic hydrogen and / or oxygen under ultravacuum conditions on removal of organic contamination from the surface.

RECOMMENDED LITERATURE:

Podle pokynů vedoucího práce.

Date of project specification: 4.2.2019 ***Deadline for submission:*** 30.5.2019

Supervisor: Ing. Ondřej Šik, Ph.D.
Consultant:

doc. Ing. Jiří Háze, Ph.D.
Subject Council chairman

VYSOKÉ UČENÍ TECHNICKÉ V BRNĚ
FAKULTA ELEKTROTECHNIKY A KOMUNIKAČNÍCH TECHNOLOGIÍ

Bakalářská práce

bakalářský studijní obor **Mikroelektronika a technologie**
Ústav mikroelektroniky

Student: Rastislav Čermák ***ID:*** 198143
Ročník: 3 ***Akademický rok:*** 2018/19

NÁZEV TÉMATU:

Studium vlastností povrchu monokrystalů CdTe se sub-nanometrovým hloubkovým rozlišením

POKYNY PRO VYPRACOVÁNÍ:

Cílem práce je studium horních vrstev polovodičového materálu CdTe po různých chemických modifikacích jeho povrchu. Pozornost je věnována srovnání působení leptadel na krystaly s orientací (111), které jsou v orientaci (111)B terminovány tellurem a v orientaci (111)A kadmiem.
Cílem studia bude posouzení vlivu expozice povrchu atomárním vodíkem a kyslíkem v podmínkách ultravaku a na stechiometrii svrchní vrstvy a na redukci jeho kontaminace organickými látkami.

DOPORUČENÁ LITERATURA:

Podle pokynů vedoucího práce.

Termín zadání: 4.2.2019 ***Termín odevzdání:*** 30.5.2019

Vedoucí práce: Ing. Ondřej Šik, Ph.D.
Konzultant:

doc. Ing. Jiří Háze, Ph.D.
předseda oborové rady

ABSTRACT

In the Central European Institute of Technology (CEITEC) laboratires, a Qtac device is available, allowing us to quantitatively measure the composition of the upper-most atomic layer of different materials, including dielectrics. Qtac uses the backscattering of low-energy ions, the so-called LEIS method. Besides the surface atomic layer analysis, using the Dynamic mode LEIS can determine the depth profile of elemental concentrations with sub-nanometer precision.

KEYWORDS

CdTe, LEIS, stochiometie, povrchová kontaminace

ABSTRAKT

V laboratořích Středoevropského technologického institutu – CEITEC je k dispozici unikátní zařízení Qtac, umožňující kvantitativně měřit složení horní atomové vrstvy různých materiálů včetně izolátorů. Qtac k tomu využívá nízkoenergiového rozptylu iontů, tzv. metodu LEIS. Kromě analýzy horní atomové vrstvy je LEIS v Dynamickém módu schopen určit hloubkový profil koncentrace prvku se sub-nanometrovým hloubkovým rozlišením.

KLÍČOVÁ SLOVA

CdTe, LEIS, stoichiometry, surface contamination

ČERMÁK, Rastislav. *Investigation of properties of CdTe single-crystals surfaces with sub-nanometer depth resolution*. Brno, Rok, 37 p. Bachelor's Thesis. Brno University of Technology, Fakulta elektrotechniky a komunikačních technologií, Ústav mikroelektroniky. Advised by Ing. Ondřej Šik, Ph.D.

DECLARATION

I declare that I have written the Bachelor's Thesis titled "Investigation of properties of CdTe single-crystals surfaces with sub-nanometer depth resolution" independently, under the guidance of the advisor and using exclusively the technical references and other sources of information cited in the thesis and listed in the comprehensive bibliography at the end of the thesis.

As the author I furthermore declare that, with respect to the creation of this Bachelor's Thesis, I have not infringed any copyright or violated anyone's personal and/or ownership rights. In this context, I am fully aware of the consequences of breaking Regulation § 11 of the Copyright Act No. 121/2000 Coll. of the Czech Republic, as amended, and of any breach of rights related to intellectual property or introduced within amendments to relevant Acts such as the Intellectual Property Act or the Criminal Code, Act No. 40/2009 Coll., Section 2, Head VI, Part 4.

Brno ....

author's signature

ACKNOWLEDGEMENT

I would like to thank my supervisor Ing. Ondřej Šik, Ph.D. for introducing me to the world of materials science, professional guidance, enormous patience and all the valuable advice. I would also like to thank my parents for their support and patience.

Brno ....

author's signature

Contents

List of Figures

Introduction

Since the inception of first semiconductor devices, new and unforseen applications of semiconducting materials were discovered. The wide spectrum of available materials with a broad range of controllable electrical properties motivates research of new manufacturing processes. One of the critical technology requirements is the ability to control composition and properties of the surface.

To obtain information about the surface, low-energy ion scattering spectroscopy (LEIS) is used as a quantitative technique. Ions accelerated to low energies (usually 1 keV – 10 keV) interact with the surface and their energy after backscattering is measured. This technique is extremely selective – it can determine the chemical structure of the upper atomic layer with only minor interference from deeper layers.[5]

Compound representing the need to find a reliable way to control the surface properties is cadmium telluride. CdTe gained attention of researchers for its wide band gap around 1,5 eV[6], predetermining it for high-energy photon detection.[3] CdTe photovoltaics is a widely used technology with considerable advantages over photovoltaics based on other compounds.[7] Many challenges present themselves in production of CdTe crystals with desired parameters, namely the precise control of correct stoichiometry[4] and crystallographic defects hindering the detection ability of ZnCdTe based detectors[9]. These defects are an unwanted feature of cutting and surface preparation[1] and can be removed using wet etching in bromine methanol. This etchant might change stoichiometry of the surface of CdTe depending on the crystallographic orientation, concentration of the etching solution and etching time.

In this thesis, surface treatment of cadmium telluride crystals using bromine methanol is examined. The first chapter gives a brief introduction to properties and usage of cadmium telluride. The second chapter provides description of basic principles of LEIS and D-LEIS. In the third chapter, practical results of CdTe stoichiometry measurements after chemical etching in bromomethanol with different contentrations are presented. D-LEIS, ARXPS, AFM and optical microscopy are used. Etch rate dependency on the concentration of bromine methanol is determined.

1 Cadmium Telluride

CdTe is a binary compound from the II-VI group that forms a crystallic structure. It is a semiconductor with the band gap energy around 1,5 eV at 300 K (different works report values ranging from 1,37 eV to 1,54 eV depending on the method used).[6] This wide band gap together with high atomic numbers (48 for Cd and 52 for Te) makes it a very perspective material for purposes of radiation detection.

Its crystallic structure is zincblende, same as diamond. Due to this structure, cutting the crystal along the (111) axis yelds two parts terminated with different predominant particles – one part is terminated with cadmium (denoted (111)A), the other one with tellurium (denoted (111)B).[4]

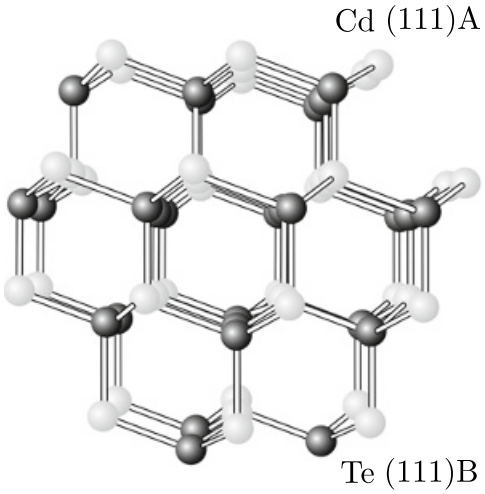

Fig. 1.1: CdTe crystal after cutting along the (111) axis.[4]

CdTe is a direct band gap semiconductor – an electron in the conduction band can directly emit a photon and transfer to the valence band, in contrast with the indirect band gap semiconductor, where an electron must transfer momentum to the crystal lattice in order to emit a photon and to move from the lowest-energy state in the conduction band to the highest-energy state in the valence band.

To tune the band gap energy to better fit the application, mercury or zinc is used forming mercury cadmium telluride (HgCdTe) or cadmium zinc telluride (ZnCdTe).

1.1 Surface treatment and defects

Surface of the semiconductor largely determines the behavior of the device it is embedded in. An incorrectly prepared surface can hinder the creation of proper ohmic

connections or growth of another crystallic layer. In the case of CdTe, surface preparation poses interesting challenges due to its soft-brittle mechanical characteristics.

The surface of the crystal can be prepared using lapping. During lapping, surface of the lapped object is rubbed against a grinding tool with abrasive between them. This process introduces a range of crystallographic defects in CdTe and ZnCdTe extending below the surface and contribute to unwanted electrical properties of the sample – for example, an unwanted avalanche breakdown can occur at lower voltages than measured in the defect-free CdTe structure.[8] Various etchant solutions can be used to determine the extent of the subsurface damage after mechanical lapping. Etch rates of these etchants depend on the structure of the crystal. Using these etching solutions, three regions with distinct types of mechanical damage after lapping were found:

- 10 μm thick almost amorphous surface layer
- severely damaged polycrystalline region with microcracks 50 μm deep
- region of plastic deformations reaching depth of 180 μm

Deeper parts of the sample show no mechanical damage.[1]

The damaged layer can be removed using wet etching. In this process, the sample is submerged in a liquid-phase etchant and due to its chemically corrosive properties, the etchant chemically removes material from the sample. The amount of material removed can be controlled by precisely limiting the time of etching or by the choice of the etchant and its concentration. Etching solutions based on elemental bromine are often used for CdTe and ZnCdTe. These solutions are more selective towards Cd and leave Te enriched surface after etching.[4]

1.2 Applications of CdTe compounds

Use in photovoltaics

The band gap energy of approximately 1,5 eV is near the theoretical optimum for band gap enery of solar cell material. This optimum was calculated as 1,36 eV (taking the possible change of the cell temperature into account)[10]. In comparison, CdTe thin film photovoltaics bests other technologies in carbon footprint size, very short energy payback and the possibility to recycle old solar cells. Efficiency of CdTe cells is around 20%.[7]

Radiation detectors

When a stream of photons with sufficient energy interacts with the semiconductor material, electron-hole pairs are generated. These free charge carriers can be extracted from the material using an electric field and registered as current passing

through the circuit. Energy of the photon necessary to generate an electron-hole pair is given by the affinity of the material.

Current through the material can be detected even if no radiation is present – this current is called *dark current* and is caused by thermally generated free charge carriers. Subsurface damage in the form of dislocation walls (mosaic structure) greatly increases dark current in ZnCdTe detectors compared to a sample without defects. This increase is attributed to weakly bound charge carriers on the dislocation walls and these walls therefore act as electrically active recombination centers.[9]

HgCdTe is used to detect infrared radiation, CdTe and ZnCdTe is used as a detecting medium for X-ray and γ radiation.[3]

2 LEIS

2.1 Brief history of ion scattering research

The first experiment involving ion backscattering from surface was the famous Geiger–Marsden experiment (also known as Rutherford gold foil experiment). In this experiment, scattering of α and β particles on a very thin golden foil was observed. The number of backscattered particles was inconsistent with the Thomson atomic model – according to this model, the atom consists of electrons floating in a uniformly positively charged volume. However, this volumetric positive charge is not sufficient to cause the backscattering observed at angles close to 180°. Based on this result, a new model of atom was proposed by Rutherford – the atom consists of a small positively charged nucleus with electrons orbiting around it.[13] This model was later replaced by the quantum mechanical model; however, the Rutherford model suffices for the description of binary nonrelativistic interactions between ion nuclei.

One of the first backscattering experiments using ions accelerated to low energies was done in 1966 by Smith. Using a simple two-body representation for the interaction of an incoming ion with an atom on the surface, the kinematics of this collision was derived. This model was tested and shown to be accurate enough to infer the composition of probed surface.[12] This technique of surface probing was called Low-energy ion scattering spectroscopy, known under the acronym LEIS.

The recent advancements in LEIS instrumentation increased the sensitivity of this technology and established it as a useful tool for surface science. One of major improvements was the double-toroidal analyser developed in 1980s. Usually, converted XPS energy analyser was used in the LEIS setup.[5] Both the analyser and XPS will be discussed in subsequent chapters.

2.2 Principles of LEIS

Low-energy ion scattering spectroscopy is a quantitative method for measuring the elemental composition of surfaces. The surface of the sample is bombarded with probing ions and the energy of backscattered ions is measured.

LEIS is only sensitive to the outermost atomic layer of the sample, while other surface probing mechanisms (for example time-of-flight secondary ion mass spectrometry (ToF-SIMS) and X-ray photoelectron spectroscopy (XPS)) are able to obtain information about first few nanometers below the surface. This imposes high demands on the purity of sample's surface – a monoatomic layer of contamination is sufficient to completely prevent most of the interaction of the probing beam with

the sample. This high sensitivity only to surface composition can be used to study the contamination as well.

Energy of the backscattered ion E_S is given by the equation

$$E_S = \left(\frac{\cos\theta + \sqrt{\left(\frac{M_S}{M_P}\right)^2 - \sin^2\theta}}{1 + \frac{M_S}{M_P}} \right)^2 E_P, \tag{2.1}$$

where E_P is the energy of the primary ion, θ the scattering angle (given by the setup of the apparatus), M_P is the mass of the primary ion and M_S is the mass of the particle the probing ion is scattered off of.[5] This equation is valid for $\frac{M_S}{M_P} \geq 1$ and under following three simplifying assumptions[12]:

- the target atom is not bound to any other atoms in the sample – the interaction times for the collision are approx. 10^{-16} s to 10^{-15} s, shorter than the characteristic lattice vibration periods (10^{-13} s), therefore this assumption is sufficiently valid
- thermal energy of the target atom is much smaller than E_P – at room temperature, vibration energy of an atom is approx. 0,04 eV, which is negligible compared to the energy of the inciding probing particle in the keV range
- transfer of electronic interaction energy can be neglected – the interactions are assumed to be purely kinetic

2.2.1 Choice of probing ions

Equation 2.1 can be used to determine the suitable mass ratio $\frac{M_S}{M_P}$ (the scattering angle θ is given by the experimental apparatus). When the ratio is too big, we are unable to discriminate between signals from elements with slightly different masses. If a relatively light element is expected to be present in the sample and we are interested in detecting it (for example C or O), lighter probing ions must be chosen.

Generally, ions of noble gases are chosen as the probing ions. They are more chemically inert compared to other elements and are less likely to bond to the surface of the sample or chemically react with the sample in other way. Another advantage is their gaseous state – this considerably simplifies the instrumentation (no evaporation of solid material needs to take place). Their disadvantage is high probability of neutralisation while interacting with the surface. To suppress the loss of signal due to neutralisation, alkali ions with lower neutralisation probability were considered and the technology is referred to as Alkali ISS.[14].

LEIS apparatus can detect only ions backscattered from the sample, the neutralised atoms do not reach the energy analyser. This also leads to higher surface sensitivity, because probing ions are neutralised with higher probability before they can exit the sample to carry any information about the bulk into the detector.

2.2.2 Interactions with the surface

Even if the acceleration energy used in LEIS (up to 10 keV) is considered low compared to other applications, it is sufficient to cause a range of different possible interactions.

The primary mode of interaction can be approximated with the model of binary elastic collision between the probing ion and an atom on the surface. If the backscattering occurs under the correct angle defined by the instrument, the ion travels into the energy analyser and is registered by the detector.

Forward scattering can also take place and the ion enters the sample. Ions of noble gases have very high probability of being neutralised and they diffuse with the remaining kinetic energy deeper into the sample. In some cases, the neutral noble gas atom can exit the sample and become ionised again. These scattered and re-ionised atoms are detected as backscattered ions with much lower energies and this signal is referred to as bulk signal. The bulk signal does not form a gaussian peak in the spectrum; it is registered as an elevated plateau instead. Heavier noble gases (Ar for example) are accelerated to lower speeds and therefore interact with the surface for longer periods of time. This leads to higher probability of neutralisation. Neutralised atom can stay on the surface, travel into the bulk, stay in the vacuum chamber to be eventually removed by the vacuum system or to be desorbed on the surface of the chamber or the sample itself.

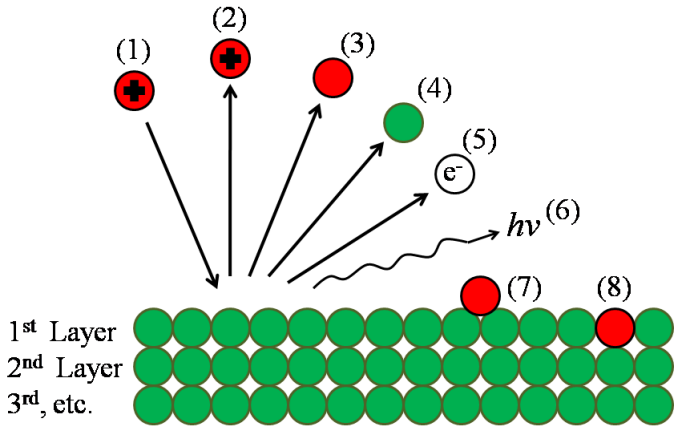

Fig. 2.1: Possible interactions of an ion with surface. (1) incoming positively charged ion; (2) ion is backscattered; (3) ion is backscattered and neutralised; (4) an atom is sputtered from the surface; (5) electron is emitted; (6) photon is emitted; (7) the ion is neutralised and stays deposited on the surface; (8) the ion is neutralised and becomes a part of the sample.

The energy of accelerated ions is sufficient to cause measurable sputtering of sample material. This sputtering is intensive enough to be used as the main mechanism for depth profiling if no sputter gun is present.

The incident ion can also generate secondary electrons. These electrons can be detected and used in the Qtac^{100} machine for additional imaging to verify the setup of the measurement and proper configuration of the system.

Electromagnetic radiation in the form of soft X-rays is generated as well. This radiation is not used for any measurement or imaging and is absorbed in the walls of the vacuum chamber, posing no threat to the operator.

2.2.3 Depth profiling and D-LEIS

Using a sputter gun, it is possible to obtain depth profile of the constituting elements. After the surface is scanned using conventional LEIS, a sputter gun is activated and the surface is bombarded with a predefined dose of ions until the desired depth for the next scan is reached. Scanning and sputtering are alternately used until the whole measurement is completed.

When a depth profile with small sputter step is necessary (as is the case in our research), no sputter gun is used – the damage from probing will uniformly remove a layer of the sample. The thickness of this removed layer depends on the mass of the ions, energy of acceleration, total dose and the material itself. The sputtering is linear with number of scans and the thickness of one layer is the ratio of number of layers and the final depth (measured using a different measuring tool). This regime is called Dynamic LEIS, or D-LEIS for short.

2.2.4 LEIS instrumentation

High vacuum is necessary for the probing ions to reach the sample and to reliably obtain information about the surface – collisions of the probing atoms with the residual atmosphere would lead to incorrect energy readouts in the analyser.

An XPS energy analyser reconfigured for positive ions was usually used for LEIS. This analyser was able to detect ions scattered only at a fixed scattering angle θ and only for a very small azimuthal range.

In 1980s, the double-toroidal analyser (schematically depicted in Fig. 2.2) was designed to allow the collection of backscattered ions from the full azimuthal range. This significantly increased the sensitivity of LEIS and shortened the aquisition times, lowering the overall damage to the sample during probing.[5]

The Qtac^{100} installed at CEITEC is able to detect ions at scattering angles $145° \pm 5°$. This further increases sensitivity, but the peaks in energy spectra are widened as a tradeoff.

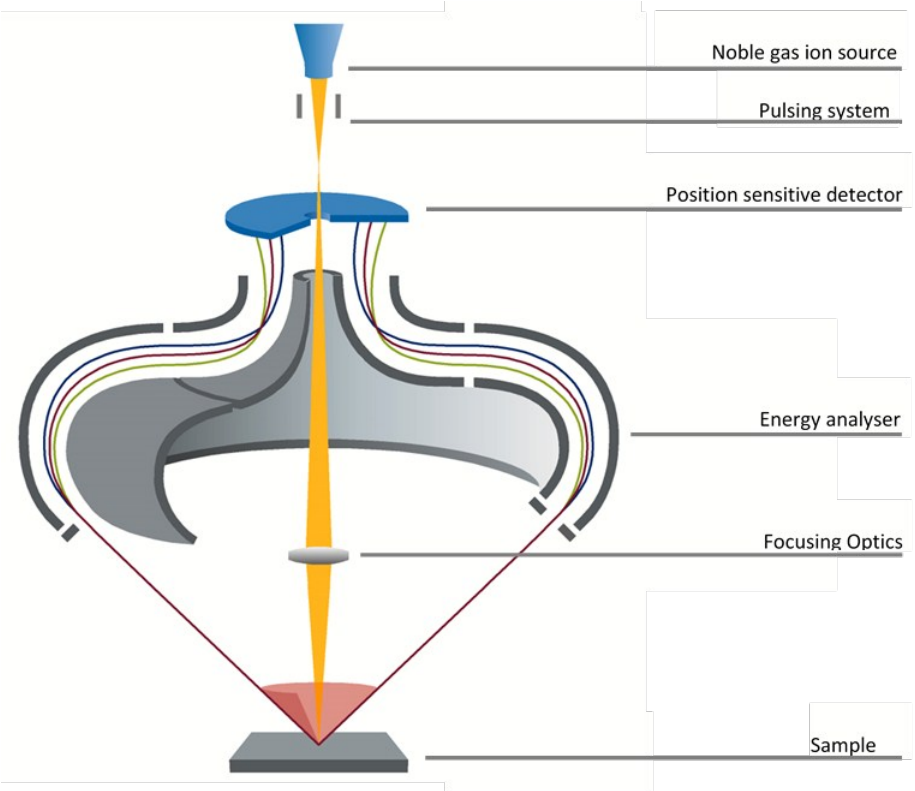

Fig. 2.2: Schematic view of the double-toroidal analyser used in the Qtac^{100} LEIS apparatus installed at CEITEC.[5]

Another possible interaction that needs to be taken into consideration is double ionisation of the probing ions. These ions are registered at lower energies in the energy analyser and can be falsely attributed to elements not present in the sample.

2.3 Other commonly used surface profiling techniques

Secondary Ion Mass Spectrometry - Time of Flight

In SIMS-ToF, the sample is bombarded with heavier positive ions that cause sputtering of the upper atomic layers. If any of the sputtered atoms is ionised, it is accelerated (typically to energies between 2 keV and 8 keV) and extracted by the secondary ion optics into an electromagnetic reflector. This device reflects the ions into the detector. Particles with lower charge-to-mass ratio spend more time in the reflector and therefore, if the detector system is capable to sample the inciding ions with sufficient frequency, one can obtain information about the sample's composition.

This method is destructive and repeated measurements conducted on the same

region of the sample can provide the depth profile of the sample.

The primary ion gun generates pulses of accelerated particles – continuous sputtering would lead to a continuous stream of particles into the detector and would make any identification of particles impossible. Lenght of these pulses is generally between 1 ns and 50 ns.

One of the advantages of this approach is the ability to detect heavier particles and even whole polymer radicals, disadvantageous are higher requirements on the detector stack – high processing speed and temporal resolution is required.[16]

X-ray photoelectron spectroscopy

X-ray photoelectron spectroscopy relies on the photoelectric effect. The sample is irradiated with X-ray photons causing external photoemission – electrons are ejected from the sample and their amount and energy is measured.

Because the X-rays can penetrate deeper into the sample and the electrons are able to escape from atomic layers under the surface, XPS obtains information about surface together with a small volume below it. The depth of this volume generally ranges from 3 to 10 nm.[15]

To get a better picture about the composition of the sample Angle Resolved XPS (ARXPS) can be used. The difference between XPS and ARXPS is in the ability to tilt the sample and irradiate it under angles lower than the right angle. The probed depth is a function of the irradiation angle – the lower the angle, the shallower is the depth, from which electrons are emitted.

The governing equation of XPS

$$E_{kin} = h\nu - E_B - \phi$$

describes the relation between kinetic energy of ejected electron E_{kin}, energy of the photon $h\nu$, work function ϕ and bonding energy of the electron E_B. E_{kin} is measured, $h\nu$ is known from the device setup, ϕ is the work function of the material. ϕ is small and almost independent of $h\nu$. E_B is calculated and, using the $E_B(h\nu)$ function, composition of the sample is inferred – the E_B of the electron is dependent on the orbital the electron originates from. Hydrogen and helium atoms cannot be practically detected due to the low probability of interaction.

Compared to LEIS, in XPS no sputtering occurs, the measurement typically takes much longer and processing and interpretation of the obtained data is much more time-demanding and requires deeper knowledge about the technique.

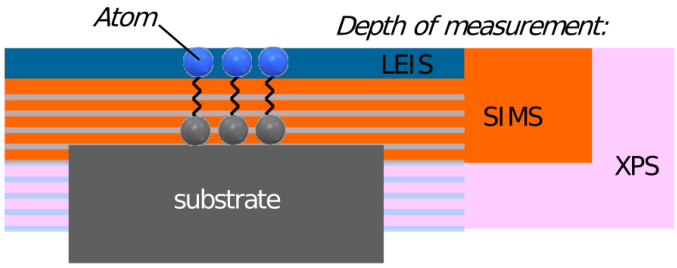

Fig. 2.3: Schematic comparison of probing depths for XPS, LEIS and SIMS. Blue vertical lines for LEIS symbolise depth profiling using a sputter gun.[15]

Atomic force microscopy

Using the AMF, one can obtain the height map of the surface of the sample. No information about the chemical composition of the sample can be obtained using AMF – only mophological features are measured.

A small cantilever with a sharp tip on its free end is lowered onto the sample, until a measurable deflection of the cantilever is observed. This method is capable of capturing images with atomic resolution.[17] The tip can be in continuous contact with the sample or a tapping mode can be used – in this mode, the tip is oscillating above the surface. Using the tapping mode, a horizontal collision of the tip with a (relatively) high morphological feature can be avoided. Schematic diagram of an AFM machine is depicted in fig. 2.4.

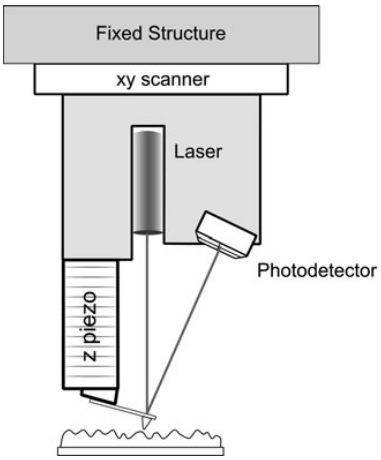

Fig. 2.4: Schematic diagram of an AFM machine. A cantilever with a sharp tip is touching the surface of the sample and the deflection of the cantilever is measured using a laser and a photodetector. Piezoelectric material in the control mechanisms allows for small and precise movements.[17]

3 Measurement of the properties of CdTe surface

Identification of (111)A and (111)B

The (111)A and (111)B sides appear identical under normal circumstances and can be identified using a reactant solution. This solution consists of hydrofluoric acid (HF), nitric acid (HNO_3) and acetic acid (CH_3COOH) in the ratio 1:1:1. After the introduction of the sample in this solution, the (111)B side becomes bright and reflecting, in great contrast to the matt (111)A side. This changed surface layer would interfere with subsequent measurements and was therefore removed by lapping to expose clean CdTe.

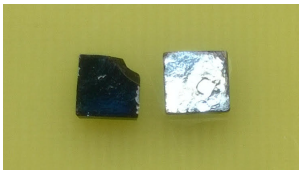

Fig. 3.1: CdTe samples after being etched in the solution used for (111)A and (111)B identification. (111)A side (left) is matt, (111)B side (right) becomes bright.

Surface preparation

Small sample of CdTe was lapped by hand because no suitable machine with the ability to generate adequate pressure was available. (The toxicity of CdTe is reported to be lower than that of pure Cd but elemental Cd can form during lapping and therefore wearing gloves is recommended.[11]) The lapping pressure was kept below 20 kPa to prevent any unnecessary damage to the sample; pressure of 20 kPa corresponds to approximately 50 g of weight. The dimensions of the sample were 5×5×1 mm. In possible future applications of CdTe in radiation detectors, thickness of 1mm is sufficient to absorb most of the photons with energy 100 keV[3].

The sample was attached to a piston with paraffin wax and inserted into a lapping jig. Lapping took place on two polishing cloths – first one (nonwoven technical textile) was used to remove any height differences on the sample and the second one (short synthetic nap) served for surface finishing. The abrasivum was Al_2O_3 powder with grain size of 3 μm. Al_2O_3 is better suited for soft-brittle CdTe than diamond powder. In the final part of the mechanical preparation, the sample was cleaned from the residual abrasive using deionised water, compressed air and ultrasound cleaning. Finally, the sample was inspected with optical microscope for any remaining defects or particles of the abrasive.

After mechanical preparation, the sample was etched in a bromine methanol solution (Br-MeOH) to remove the damaged surface layer. Because of the high surface-selectability of LEIS, caution was used not to contamine the surface while manipulating with the etched sample. Due to the desorption of airborne chemicals and particles, all contamination could not be completely eliminated.

Measurement in the Qtac^{100} LEIS machine

After preparation, the sample was introduced into the Qtac^{100} LEIS machine. The sample was fixed on a sample holder and a small metal grounding rod was attached to prevent any accidental charge buildup from the primary ions. (This is not a systemic issue of the LEIS method and was done only as a precaution.) The Qtac^{100} machine was designed with quick main vacuum chamber access in mind – the sample passes through three vacuum chambers to minimise the amount of atmosphere entering the main vacuum chamber. After the sample was inserted into the load lock chamber, it was evacuated until the pressure stabilised. It was then transferred into the second chamber with better vacuum system and stayed there until the pressure stabilised again and the sample could continue to the main chamber.

Ion current was adjusted with the change of the parameters of ion optics and measured using a Faraday cup on the sample holder. Faraday cup is a device for measurement of ion beam current – it is a small opened chamber, that is able to catch backscattered ions, that would not contribute to the measured current. Z-coordinate of the sample holder was adjusted manually using the built-in homing laser. After a suitable area on the sample was chosen, the measurement in the Dynamic mode was started.

The CdTe sample was relatively small and required no heating during the experiment, thus no outgassing from the sample was taken into consideration. No desorption of the residual atmosphere in the chamber was expected, because the aquisition times were short and samples were not left in the chamber for longer periods of time.

3.1 LEIS and D-LEIS

Using the D-LEIS method, a number of LEIS spectra was taken, every spectrum coming from a deeper layer in the sample. In this measurement, we are using the fact that no preferential sputtering towards Cd or Te occurs. Data from the regions near the edges of the sputtered pit might be incorrect because of possible interactions of ions with the walls of the pit and were discarded using the Qtac^{100} software.

The surface was probed using Ne^+ ions accelerated to 5 keV. The ion dose was chosen to be $2 \cdot 10^{14}$ ions/cm^{-2}, which corresponds to $\approx$ 0,4 nm of sputtered material per one spectrum. The dimensions of the scanned area were 600×600 μm. For illustration, spectra from surface, layer 10 and layer 44 are shown on Fig. 3.2. In the first spectrum, signals from Cd and Te are weak because of the impurities on surface. In layer 10, we can see Te peak on the right already reaching its maximum and Cd peak on the left being lower than deeper in the bulk – this is due to etchant selectability towards Cd. Layer 44 was measured deep in the bulk and the stoichiometry of CdTe is 1:1.

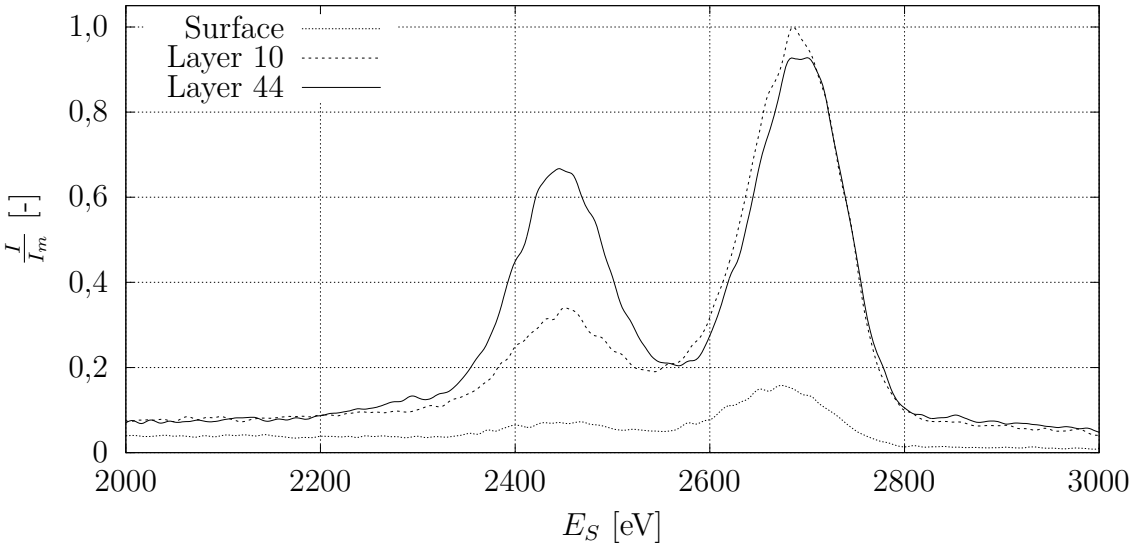

Fig. 3.2: LEIS spectra from different depths of the sample. Peak on the left is Cd, right peak corresponds to Te. This sample was etched in the 5% solution of Br. Because only relative values in this measurement are relevant, the spectra are normed by the maximal value.

Using the Qtac^{100} software, measured spectra were fitted with the spectra of pure Cd and Te etalons. In the first approach, a Python script was used to fit Gaussian peaks to the spectra, but due to the nature of the measured peaks, the fitting error was high. The fitting error would be lower using the Voigt profile, but by using the measured spectra of pure Cd and Te, different isotopes and the bulk signal are taken into account as well.

The change of Cd and Te peak area with increasing depth is in Fig. 3.3. From these data, we can calculate the Te/Cd ratio, as can be seen in Fig. 3.4. The measured stoichiometry of CdTe in Fig. 3.4 deep in the bulk is not 1:1 – this is because *shadowing* occurs. Shadowing depends on the crystallographic orientation and in our case, primary ions are more likely to react with Te than with Cd. Because

the stoichiometry in bulk is 1:1, the data were normed to reflect this fact in Fig 3.5. Etchant selectability towards Cd is clearly visible in the surface region.

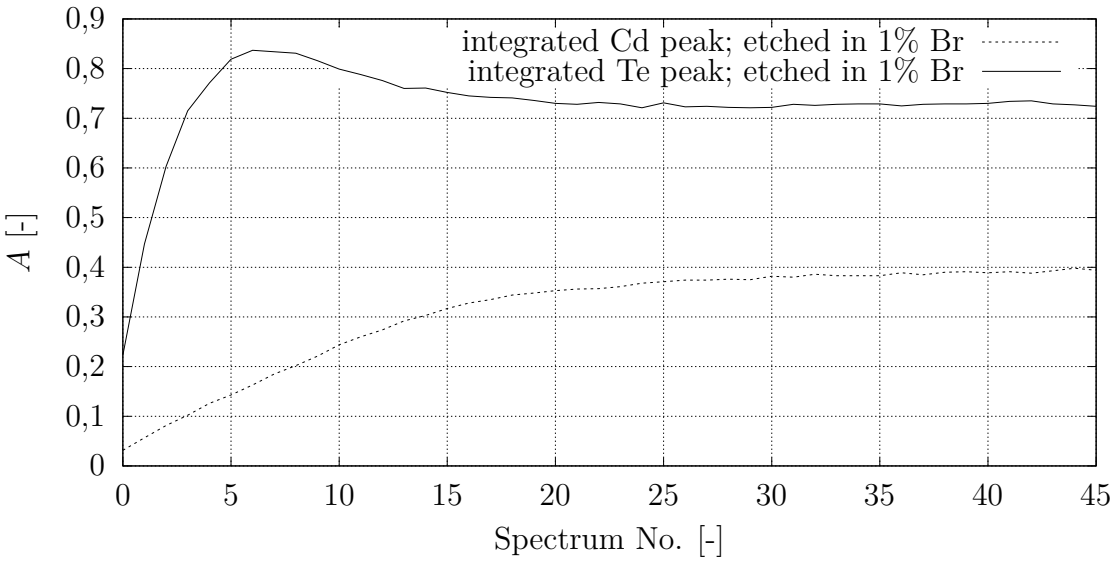

Fig. 3.3: Integrated Cd and Te peaks. Raw data obtained from every LEIS spectrum corresponding to Cd and Te peaks were fitted using the Cd and Te spectra and then numerically integrated.

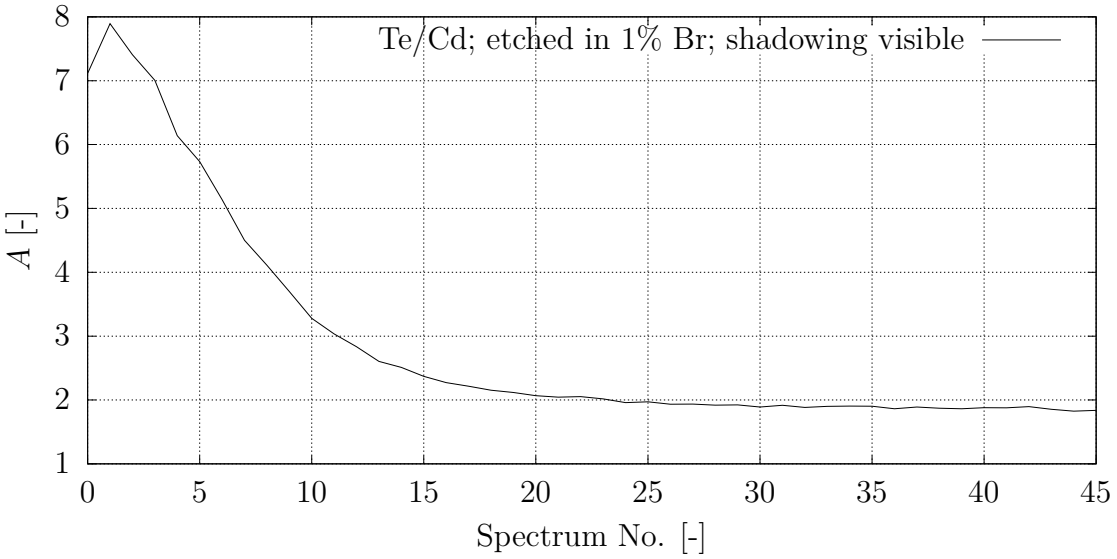

Fig. 3.4: Te/Cd ratio of the integrated raw data. Apparent stoichiometry in the bulk is not 1:1. This is probably due to an effect called *shadowing* – in this case, primary ions interact with Te with higher probability. This effect is dependent on the crystallographic orientation.

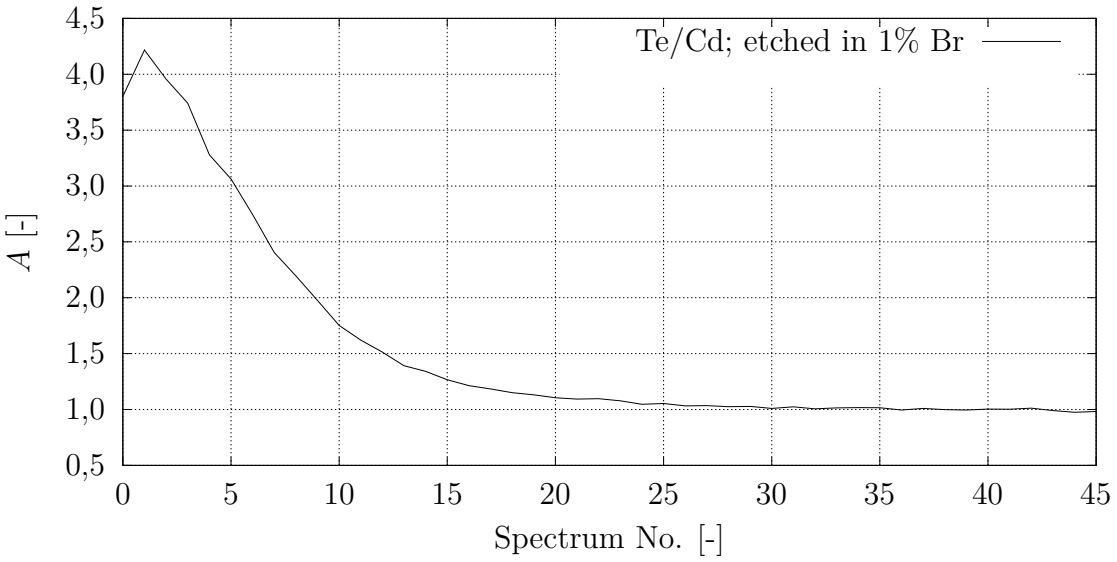

Fig. 3.5: Te/Cd ratio for sample etched in 1% solution. The etching solution preferentially removes Cd. The data were normalised to form a 1:1 Te/Cd stoichiometry deep in the bulk.

3.1.1 CdTe etched in Br-MeOH

D-LEIS measurements were conducted on the (111)A and (111)B side after etching in Br-MeOH.

Te/Cd depth profile for (111)A is depicted in Fig. 3.6. Each CdTe sample was etched in one of the Br-MeOH solutions with 0,5%, 1%, 2% and 3%. Selectivity towards Cd varies with concentration – for the first layer, Te/Cd ratio for 0,5% is 4,769 and 7,446 for 2%. No signal from Cd was present in the first layers of samples etched in 1% and 3% solutions, therefore the Te/Cd ratio was impossible to determine.

The Te/Cd ratio for (111)B is in Fig. 3.7. Again, four CdTe samples were etched for one minute in Br-MeOH solutions with concentrations 0,5%, 1%, 3% and 7%. The etchant clearly leaves Te-enriched surface and the Te/Cd ratio does not depend strongly on the concentration. The 7% Br-MeOH is slightly less selective towards Cd and the stoichiometry returns to 1:1 after approx. 10 measured spectra.

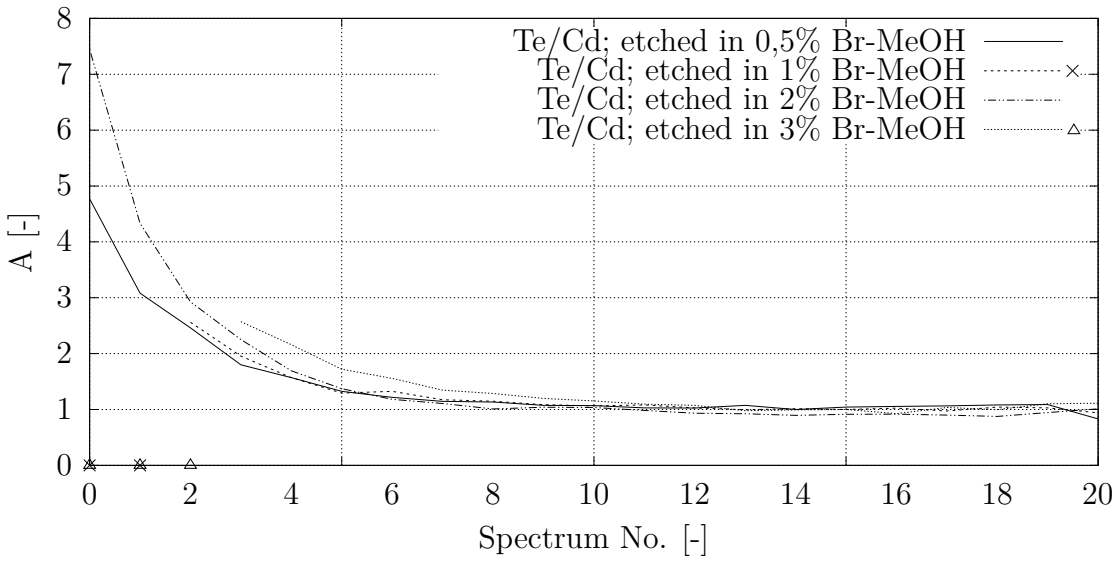

Fig. 3.6: Te/Cd ratio for (111)A sample etched in 0,5%, 1%, 2% and 3% solution of Br-MeOH. The etching solution preferentially removes Cd in all cases. For samples etched in 1% and 3%, no Cd signal was present in the first 2, resp. 3 layers. This is represented by crosses and triangles in the graph. The data were normalised to form a 1:1 Te/Cd stoichiometry deep in the bulk.

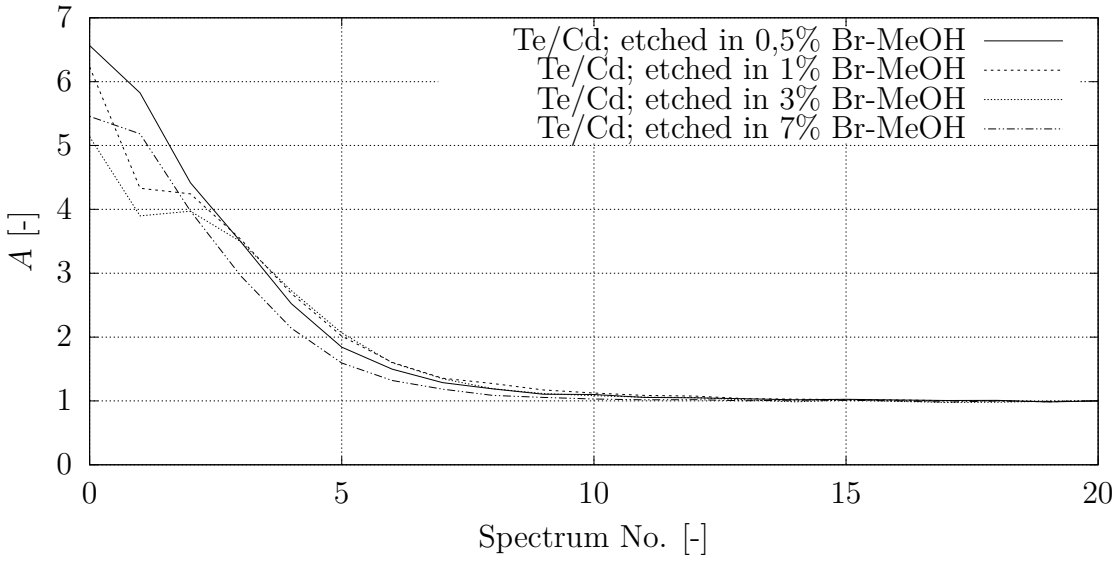

Fig. 3.7: Te/Cd ratio for (111)B sample etched in 0,5%, 1%, 3% and 7% solution. Cd is removed from the surface in both cases. The data were normalised to form a 1:1 Te/Cd stoichiometry deep in the bulk.

3.1.2 Surface profiling using He^+ ions

After measuring with Ne^+, He^+ ions were selected to qualitatively measure the impurities on the surface. At the Qtac^{100} at CEITEC, a single gas cylinder with helium-neon mix is installed. The desired gas is selected in the Qtac^{100} software by changing the configuration of the analyser gun. Acceleration voltage was lowered to 3 kV because of the smaller mass of He^+. LEIS spectrum from the surface next to the probed area is in Fig. 3.8. No peak that could be attributed to either Cd or Te is visible – the impurities with lower atomic mass completely block any interaction with CdTe. These impurities, namely carbon, are residuals commonly found on surfaces etched in Br-MeOH.[2] Signal plateau between 1500 eV and 2500 eV might be partly the bulk signal from CdTe below the surface.

Spectrum from the probed area is in Fig. 3.9 – no impurities remain, only CdTe is detected. Due to the limitations of LEIS with He^+ only one narrow peak is detected.

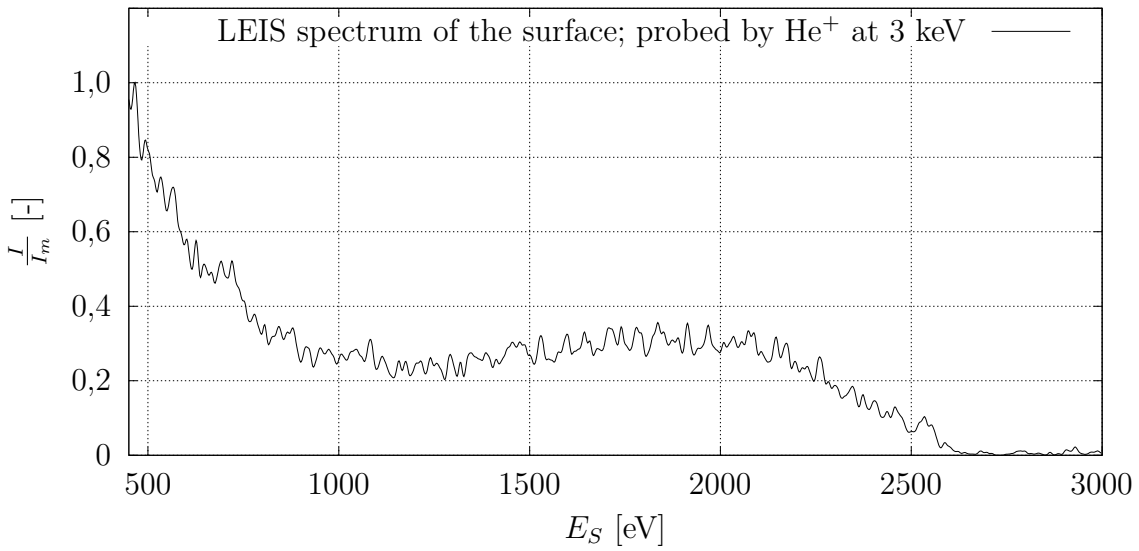

Fig. 3.8: LEIS spectrum of CdTe surface before sputtering. No peaks corresponding to Cd and Te around 2600 eV are present – the impurities prevent any interaction between primary ions and the bulk. Data are normalised by the maximum value.

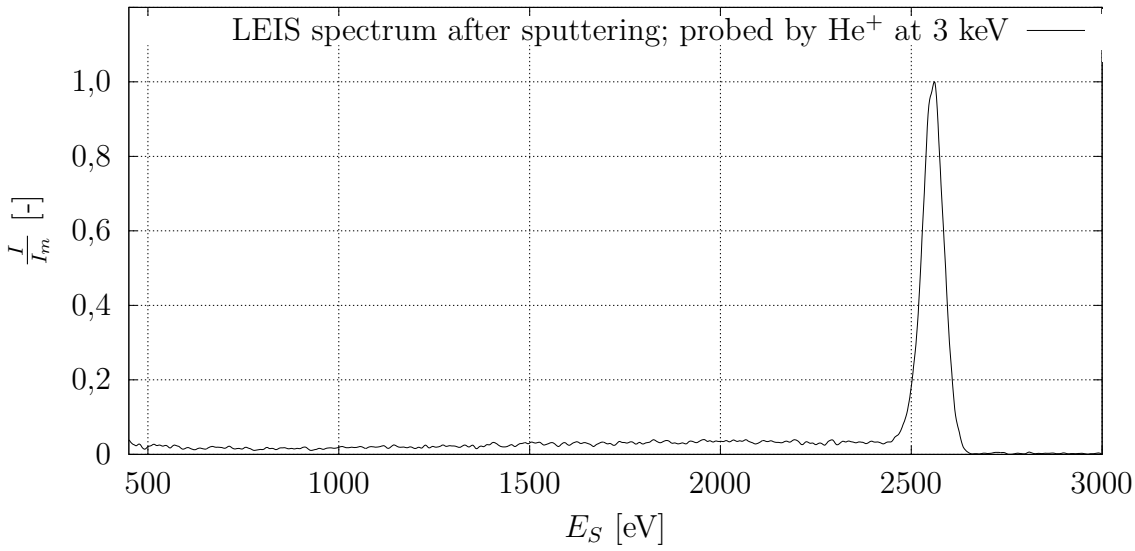

Fig. 3.9: LEIS spectrum of CdTe surface after sputtering. No signal from impurities is present. The peaks corresponding to Cd and Te are combined into one because of the small weight of He^+ ions – according to 2.1, the energy difference between Cd and Te peaks is around 40 eV, which is below the detection capabilities of LEIS. Data are normalised by the maximum value.

3.2 ARXPS

Before the destructive D-LEIS measurement, the same samples were profiled by ARXPS. The measurement and data processing was done by Ing. Ondřej Šik, PhD.

The ARXPS dataset corresponds to the D-LEIS dataset. On both sides, the upmost layers of the sample (corresponding to $\varphi = 70°$) are Te-enriched. In the case of the (111)A side, different Te/Cd rates for different Br-MeOH concentrations were measured. No visible relation between the Te/Cd and the concentration of the etchant for the (111)B side was discovered.

The stoichiometry did not reach 1:1 for the angle $\varphi = 0°$ (when the signal comes from the deeper region of the sample), because electrons from the Te-enriched surface were registered as well.

The depth profile of Te/Cd obtained from ARXPS for side (111)A is in Fig. 3.10, for side (111)B in Fig. 3.11.

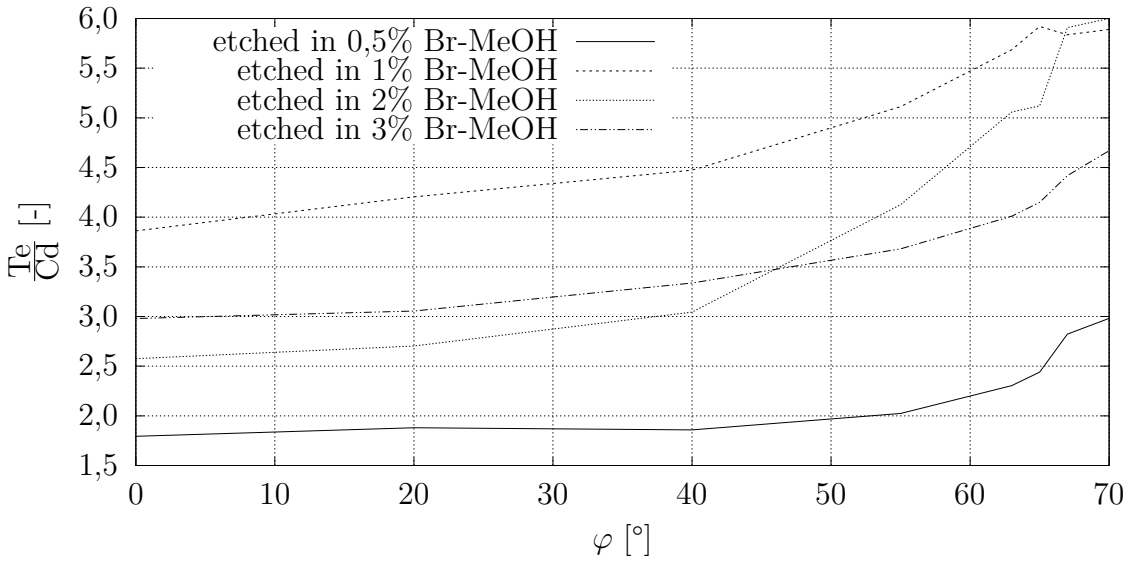

Fig. 3.10: Te/Cd in (111)A measured using ARXPS. High angles φ correspond to the topmost layers of the sample. Br-MeOH is selective towards Cd.

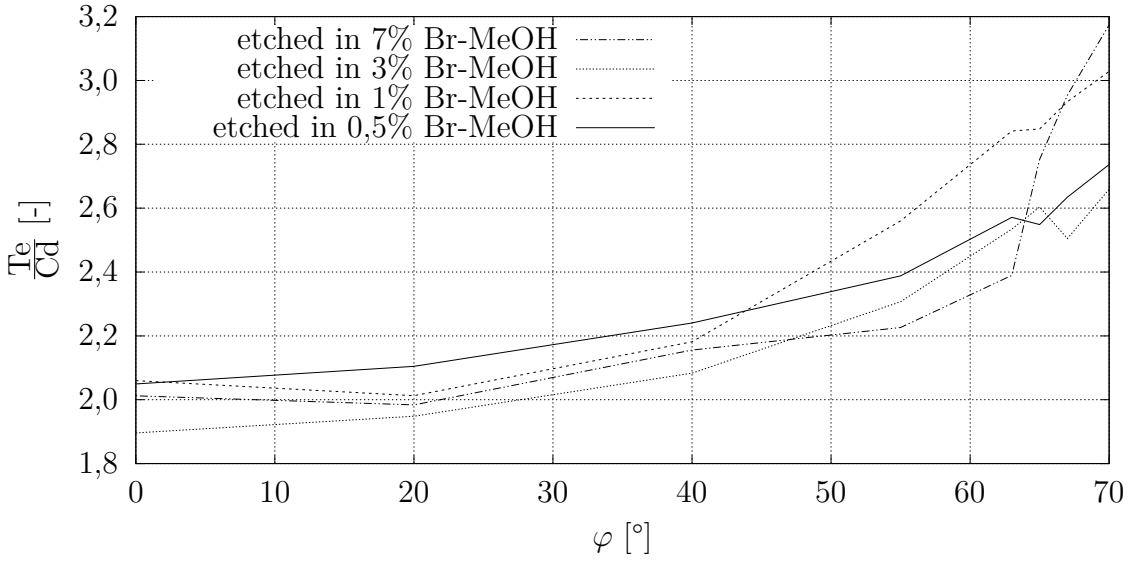

Fig. 3.11: Te/Cd in (111)B measured using ARXPS. High angles φ correspond to the topmost layers of the sample. Measured data correspond to D-LEIS data – Br-MeOH is selective towards Cd with almost no dependency on the concentration.

3.3 Surface morphology of etched CdTe

Another quantitative and qualitative insight into the preparation of CdTe surface using Br-MeOH offers AFM and optical microscopy. Optical images were taken using the Carl Zeiss Observer Z1[19]. To highlight the morphological features, differential interference contrast mode (DIC) was used.

For AFM imaging, the Bruker Dimmension Icon microscope[20] with the Scan Assist tip was used. Scanned area was 20x20 μm with scanning frequency 0,6 Hz. First, a small area was scanned using 128x128 points at three different places on the sample to check the validity of the measurement and a more detailed scan with 765x765 points was taken afterwards.

Both sets of pictures were taken by Ing. Ondřej Šik, PhD. Gwyddion software[18] was used for processing of the AFM data.

3.3.1 Optical and AFM imaging

The surface of CdTe after lapping is visibly scratched in the picture from the optical microscope in Fig. 3.12.

Optical microscopy (Fig. 3.13) revealed visible scratches on the surface of the sample etched in 0,5% Br-MeOH on both sides. With higher concentrations, the scratches are less prominent and more black dots appear – these are areas with heightened concentrations of tellurium.

Similar evolution of morphological features with changing etchant concentrations can be seen in the AFM pictures (Fig. 3.14). Scanning resolution in the sub-micron range enables us to see the disappearance of the smaller scratches after etching with higher concentrations of Br-MeOH.

Fig. 3.12: Optical image of the CdTe surface before any etching – surface grooves caused by the lapping are clearly visible.

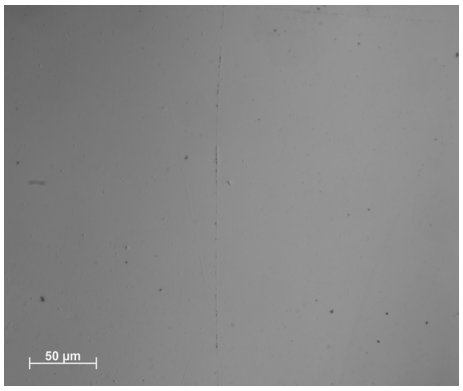

(a) (111)A in 0,5% Br-MeOH

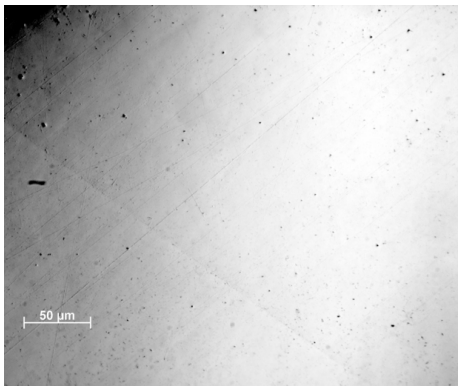

(b) (111)B in 0,5% Br-MeOH

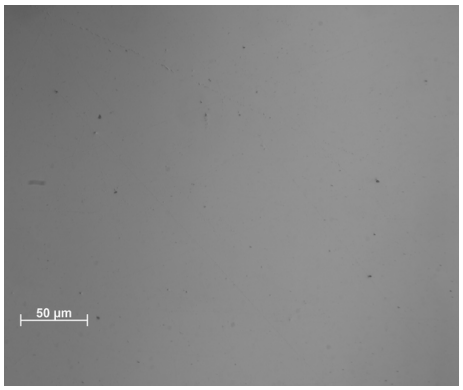

(c) (111)A in 1% Br-MeOH

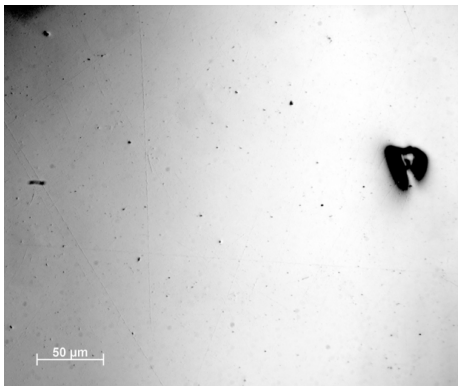

(d) (111)B in 1% Br-MeOH

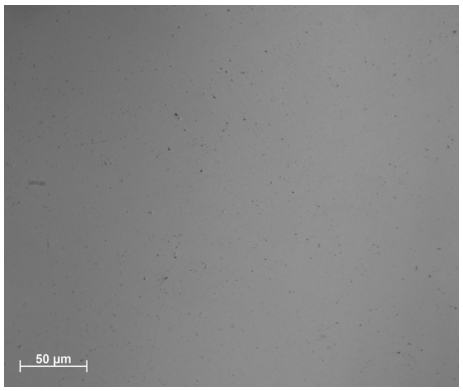

(e) (111)A in 2% Br-MeOH

(f) (111)B in 2% Br-MeOH

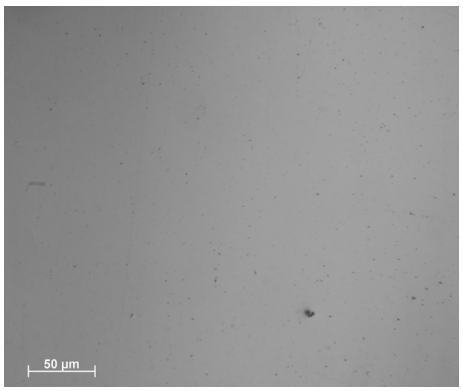

(g) (111)A in 3% Br-MeOH

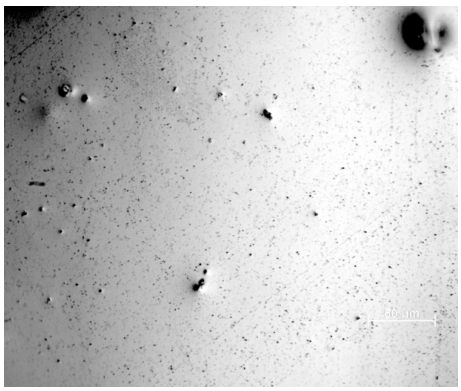

(h) (111)B in 3% Br-MeOH

Fig. 3.13: Optical images of the surface of CdTe after etching in Br-MeOH.

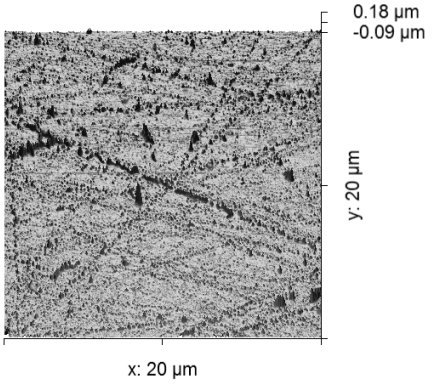

(a) (111)A in 0,5% Br-MeOH

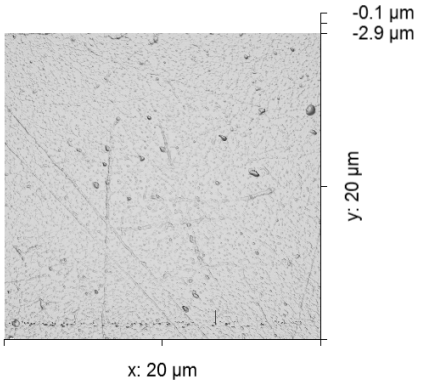

(b) (111)B in 0,5% Br-MeOH

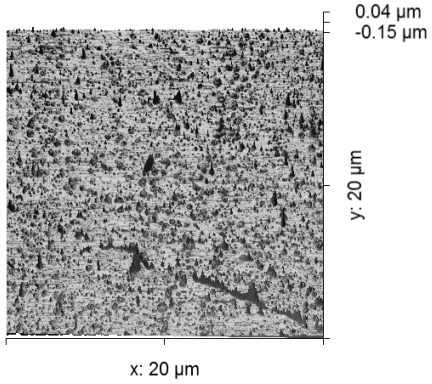

(c) (111)A in 1% Br-MeOH

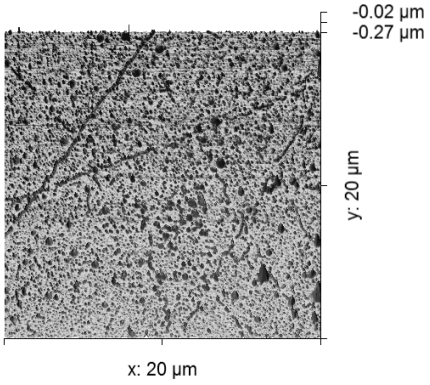

(d) (111)B in 1% Br-MeOH

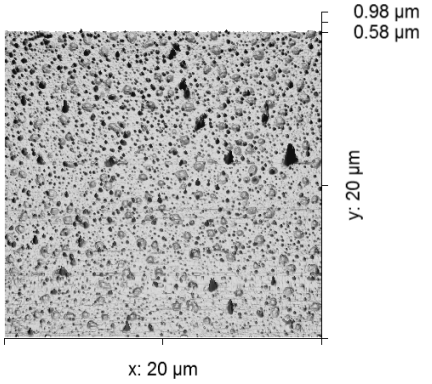

(e) (111)A in 2% Br-MeOH

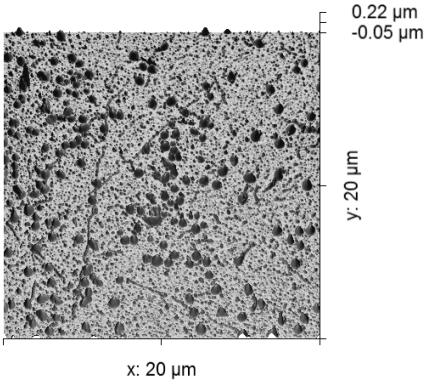

(f) (111)B in 2% Br-MeOH

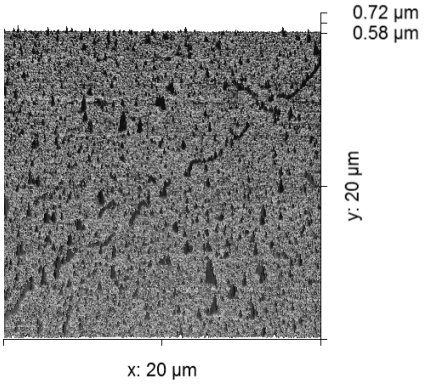

(g) (111)A in 3% Br-MeOH

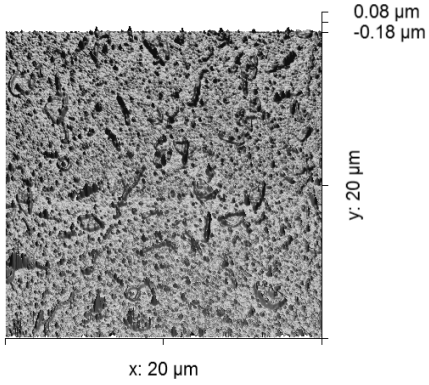

(h) (111)B in 3% Br-MeOH

Fig. 3.14: AFM images of the surface of CdTe after etching in Br-MeOH.

3.3.2 Etch rate

Four samples of CdTe were prepared by lapping and a part of every sample was covered with solution of polystyrene in xylene. After the xylene has evaporated, a protective coating on the sample was formed. Prepared samples were then etched in solutions of Br-MeOH with different concentrations, namely 0,5%, 1%, 2% and 3%. The samples were etched for 60 seconds and rinsed immediately after.

The polystyrene was removed by xylene and the height difference between etched and protected part of the surface was measured using the DektakXT profiler. In this profiler, a moving stylus is in contact with the sample and the vertical displacement of the stylus during its movement is recorded.

On most of the profiles, a noticeable undercut is present. This is due to the prolonged exposure of the sample to the etchant on the places, where rinsing was not effective enough. The measured depth of the etching was taken further from the undercut pit. The surface profiles of side (111)A are in fig. 3.15 and for side (111)B in fig. 3.16.

The graph of dependency of etch rate on the concentration of the etchant is in Fig. 3.17. Etch rate is linear with concentration of the etchant and differs for (111)A and (111)B only slightly.

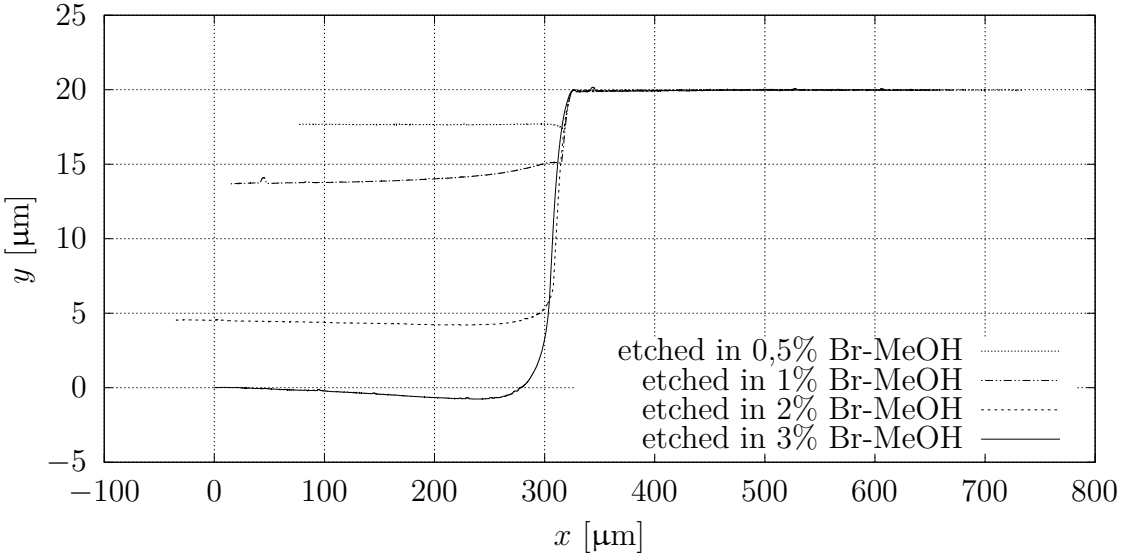

Fig. 3.15: Surface profiles of CdTe (111)A after etching in Br-MeOH solutions with different concentrations (0,5%, 1%, 2% and 3%) for 1 minute.

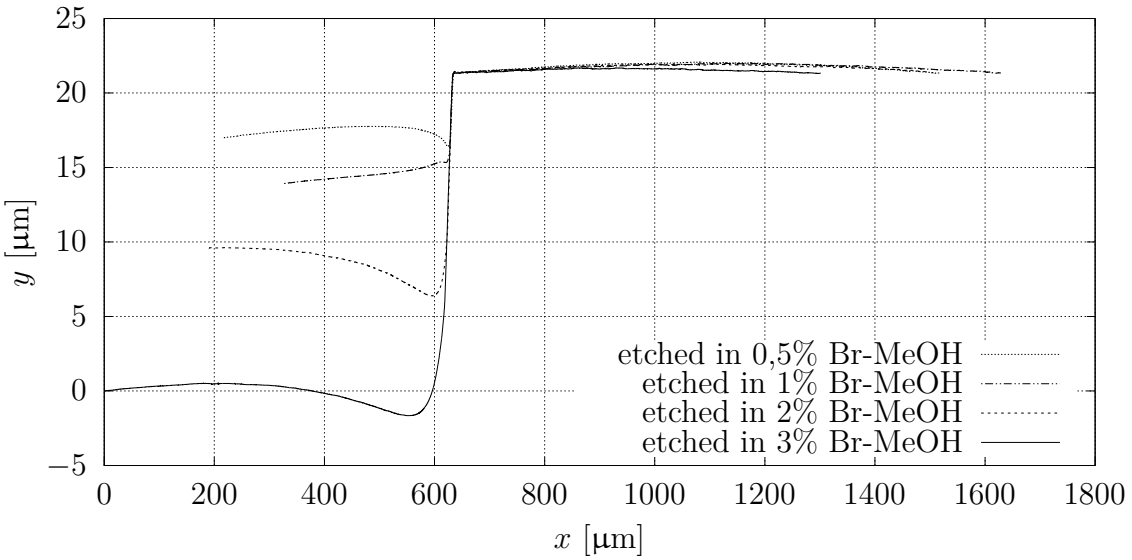

Fig. 3.16: Surface profiles of CdTe (111)B after etching in Br-MeOH solutions with different concentrations (0,5%, 1%, 2% and 3%) for 1 minute.

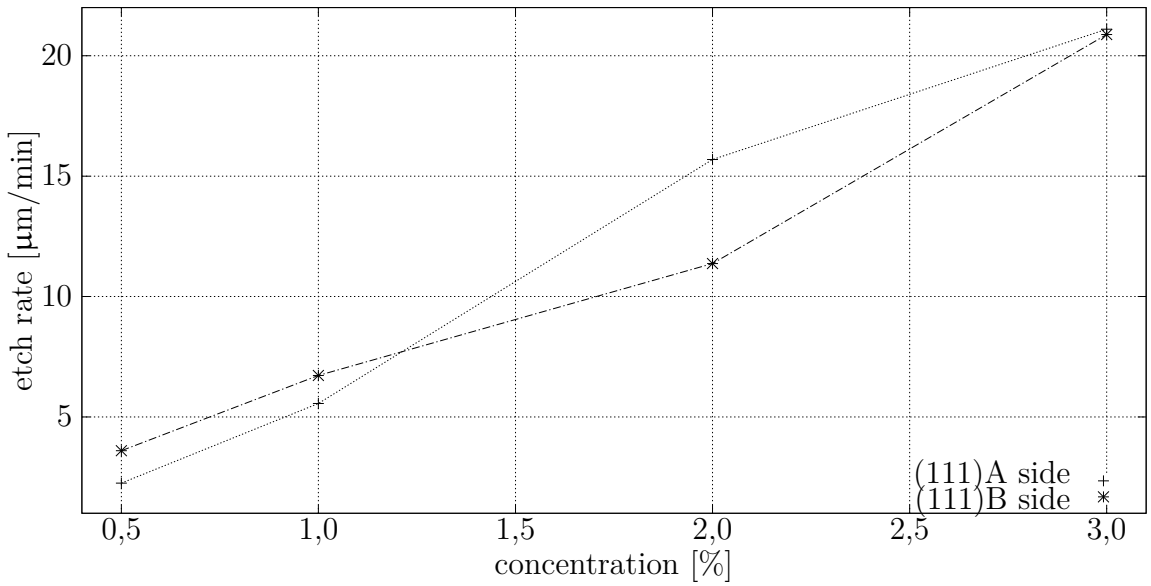

Fig. 3.17: Etch rates of CdTe in Br-MeOH solutions with different concentrations (0,5%, 1%, 2% and 3%). For both sides ((111)A and (111)B) the etch rates are approximately linear with the concentration of the etching solution.

4 Conclusion

In this work, a brief survey of CdTe and its applications was conducted. Basic principles of low-energy ion scattering spectroscopy (LEIS) were described and other surface profiling techniques were discussed.

Using the Qtac^{100} LEIS apparatus at CEITEC, depth profiles of CdTe samples etched with bromine methanol solutions were measured and compared. LEIS was used in the Dynamic mode – primary ions were used to sputter the surface and measure deeper layers of the sample. Bromine methanol changed the stoichiometry of CdTe in the surface region of the sample. In the case of (111)A, dependence of the Te/Cd ratio in the surface region of the sample was observed – etchant with higher concentration was able to remove more Cd from the sample, leaving a Te-enriched volume. For (111)B, the Te/Cd ratio was independent on the concentration of the etchant.

Surface of the sample was probed to evaluate the presence of impurities using He^+ ions. No signal form CdTe was observed, indicating at least a monoatomic layer of impurities. These impurities are with high probability the remnants of the etchant solution.

Data obtained by D-LEIS were compared with data from ARXPS. Independence of the Te/Cd ratio on the (111)B was observed.

The effectivity of removing the surface defects was examined using AFM and optical microscopy. Deeper grooves in the CdTe surface caused by lapping were more effectively removed with higher concentrations of the etchant.

Etch rate of bromine methanol on CdTe was measured. The etch rate is linear with etchant concentration and does not depend on the crystallographic orientation.

Bibliography

[1] Šik O., Škvarenina L., Caha O., Moravec P., Škarvada P., Belas E., Grmela L. *Determining the sub-surface damage of CdTe single crystals after lapping.* Journal of Materials Science: Materials in Electronics, 2017. DOI:10.1007/s10854-018-9002-7

[2] Šik O., Bábor P., Polčák J., Belas E., Moravec P., Grmela L., Staněk J., *Low Energy Ion Scattering as a depth profiling tool for thin layers - Case of bromine Methanol etched CdTe* Vacuum, 2018 DOI: 10.1016/j.vacuum.2018.03.014

[3] Del Sordo S., Abbene L., Caroli E., Mancini A. M., Zappettini A., Ubertini P. *Progress in the Development of CdTe and CdZnTe Semiconductor Radiation Detectors for Astrophysical and Medical Applications* Sensors 2009, 9(05), 3491-3526; DOI:10.3390/s90503491

[4] Triboulet R., Siffert P. *CdTe and Related Compounds: Physics, Defects, Hetero- and Nano-Structures, Crystal Growth, Surfaces and Applications.* Elsevier, 2010. ISBN: 978-0-08-046409-1

[5] Cushman C. V., Brüner P., Zakel J., Major G. I., Lunt B. M., Grehl T., Smith N. J., Linford M., *Anal. Methods*, 2016, DOI:10.1039/C6AY00765A

[6] Fonthal G., Tirado-Mejia L., Marin-Hurtado J.I., Ariza-Calderón H., Mendoza-Alvarez J.G. *Temperature dependence of the band gap energy of crystalline CdTe.* Elsevier, 2000. DOI:10.1016/S0022-3697(99)00254-1

[7] Peng J., Lu L., Yang H. *Review on life cycle assessment of energy payback and greenhouse gas emission of solar photovoltaic systems.* Elsevier, 2013. DOI:10.1016/j.rser.2012.11.035

[8] Fu X., Xu Y., Xu L., Gu Y., Jia N., Bai W., Zha G., Wang T., Jie W. *Indentation-introduced dislocation rosettes and their effects on the carrier transport properties of CdZnTe crystal* Royal Society of Chemistry, 2016. DOI:10.1039/c6ce00519e

[9] Zeng D., Jie W., Wang T., Zha G., Zhang J. *Effects of mosaic structure on the physical properties of CdZnTe crystals* Nuclear Instruments and Methods in Physics Research A 586 (2008) 439–443 DOI:10.1016/j.nima.2007.12.033

[10] Zdanowicz T., Rodziewicz T., Zabkowska-Waclawek M. *Theoretical analysis of the optimum energy band gap of semiconductors for fabrication of solar cells for applications in higher latitudes locations.* Elsevier, 2004. DOI:10.1016/j.solmat.2004.07.049

[11] Kaczmar S., *Evaluating the read-across approach on CdTe toxicity for CdTe photovoltaics*. Society of Environmental Toxicology and Chemistry (SETAC) North America. 2011

[12] Smith, D. P. *Scattering of Low-Energy Noble Gas Ions from Metal Surfaces* Journal of Applied Physics, 38(1), 340–347. DOI:10.1063/1.1708979

[13] Rutherford E., *The Scattering of α and β Particles by Matter and the Structure of the Atom* Philos. Mag, 6, 21

[14] Oura K., Lifshits V. G., Saranin A. A., Zotov A. V., Katayama M. *Surface Science, An Introduction* Springer, 2003 ISBN: 3-540-00545-5

[15] Calipso Handout, *Expertise center for High Sensitivity Low Energy Ion Scattering*[online], 2007, [cit. 10. 12. 2018] Retrieved from: <`http://calipso.nl/media/pdf/handout%202007.pdf/`>.

[16] Friedbacher G., Bubert H. *Surface and Thin Film Analysis a Compendium Of Principles, Instrumentation, and Applications* Wiley-vch Verlag, 2011 ISBN: 978-3-527-32047-9

[17] Eaton P., West P. *Atomic Force Microscopy* Oxford University Press, 2010 ISBN: 978-0-19-957045-4

[18] Nečas D., Klapetek P., *Gwyddion: an open-source software for SPM data analysis* Open Physics, 2012 DOI:10.2478/s11534-011-0096-2

[19] Zeiss, *Axio Observer for Materials* retrieved 29.5. from `https://www.zeiss.com/microscopy/int/products/light-microscopes/axio-observer-for-materials.html`

[20] Bruker, *Dimension Icon Overview – Performance AFMs* retrieved 29.5. from `https://www.bruker.com/products/surface-and-dimensional-analysis/atomic-force-microscopes/dimension-icon/overview.html`

List of symbols, physical constants and abbreviations

CEITEC	Central European Institute of Technology
LEIS	low-energy ion scattering spectroscopy
ISS	ion scattering spectroscopy
E_P	energy of the primary ion
E_S	energy of the backscattered/secondary ion
θ	scattering angle
M_P	mass of the primary ion
M_S	mass of the target particle
ToF-SIMS	time-of-flight secondary ion mass spectrometry
XPS	X-ray photoelectron spectroscopy
ARXPS	Angle resolved X-ray photoelectron spectroscopy
AFM	Atomic force microscopy
E_{kin}	kinetic energy of the ejected electron
h	Planck constant
ν	frequency of a photon
ϕ	work function
E_B	electron bonding energy